ACS OMEGA

http://pubs.acs.org/journal/acsodf

Article

Elucidation of Iron(III) Bioleaching Properties of Gram-Positive Bacteria

Hao Jing, Zhao Liu, Jun Chen,* and Chun Loong Ho*

Cite This: *ACS Omega* 2022, 7, 37212−37220

Read Online

ACCESS | Metrics & More | Article Recommendations | Supporting Information

ABSTRACT: Microbial-based iron reduction is an emerging technology used as an alternative to conventional chemical-based iron reduction. The iron reduction in kaolin refinement is vital for enhancing its commercial value. Extensive studies on microbial-based iron reduction mainly focus on Gram-negative bacteria, whereas little is understood about Gram-positive bacteria's mechanism and potential application. This study aims to investigate the iron-reducing mechanism of two Gram-positive bacterial isolates, *Bacillus cereus* (*B. cereus*) and *Staphylococcus aureus* (*S. aureus*). By varying the growth environment of bacteria and monitoring the biochemical changes during the process of iron reduction, the results show that Gram-positive bacterial iron reduction performance depends on the medium composition, differing from Gram-negative bacteria-based reduction processes. Nitrogen-rich medium facilitates the microbial basification of the medium, where the alkaline conditions impact the microbial iron reduction process by altering the gene expression involved in intracellular pH homeostasis and microbial growth. This discovery will contribute to the mineral refining processes and promote the development of microbial-based bioprocesses for ore purification, while also laying the foundation for investigating other Gram-positive bacterial iron-reducing ability.

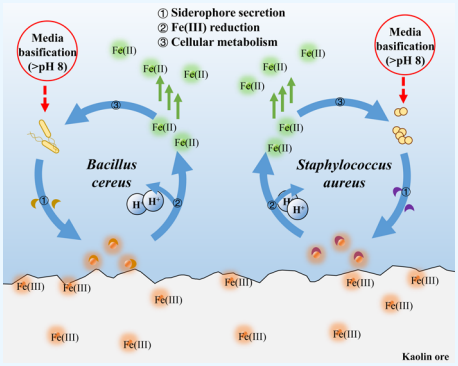

INTRODUCTION

Kaolin is a silicate clay mineral exhibiting excellent physical and chemical properties and used primarily in papermaking, refractory materials, rubber, ceramics, plastic, coatings, and other industrial fields.[1,2] However, the iron contaminants in unprocessed kaolin ores reduce the whiteness of kaolin, limiting its industrial and pharmaceutical applications.[1,3] As an alternative to traditional physical- and chemical-based iron leaching processes, microbial-based processes are deemed advantageous due to their lower operational cost and environmentally sustainable approach.

Various studies found that some microorganisms extract iron oxides (the predominant form of iron-based contaminants) in kaolin clay by producing organic acids. *Aspergillus niger* can facilitate iron contaminant removal in kaolin ore, achieving industrial grade purity applicable for papermaking, coatings and fillers.[4] This microbial-based leaching process outperforms conventional bleaching methods by increasing the kaolin ore whiteness by over 50%, while generating lesser chemical waste.[5] However, the use of *A. niger* is limited as it generates an acidic environment during the leaching processes that can impact the environment. Other iron oxide extraction approaches use other iron-respiring bacteria such as Gram-negative *Shewanella* that reduce ferric(III)oxide to ferrous ions through electron transfer during microbial growth.[6−9]

Currently, limited Gram-positive bacteria are found to possess the iron leaching capabilities, impeding the understanding of the iron-leaching mechanism in these bacteria. Therefore, this study aims to investigate the ferric(III)oxide leaching mechanism of two Gram-positive bacteria under different growth conditions, and the different biochemical responses that occur throughout the bioleaching processes.

MATERIALS AND METHODS

Materials and Strains. All bacterial culture reagents were purchased from Oxoid (Basingstoke, Hampshire, United Kingdom), Macklin (Shanghai, China) and Aladdin (Shanghai, China). Biochemical reagents were purchased from Aladdin (Shanghai, China), Macklin (Shanghai, China) and Shanghai lingfeng chemical reagent Co., LTD (Shanghai, China). Raw kaolin was acquired from the local Chinese mines in Jiangxi Province, China.

Microbial strain *Bacillus cereus* UKMTAR-4 was acquired as a gift from Sylvia Chieng, Universiti Kebangsaan, Malaysia. *Staphylococcus aureus* NCTC 6571 (from ATCC 9144) was acquired from the in-house microbial bank.

The prepared medium included lysogeny broth, LB (10 g of tryptone, 5 g of yeast extract, and 10 g of sodium chloride per

Received: June 1, 2022
Accepted: October 7, 2022
Published: October 17, 2022

liter); 10× diluted lysogeny broth, 0.1LB (1 g of tryptone, 0.5 g of yeast extract, and 1 g of sodium chloride per liter); glucose medium (15 g of glucose, 10 g of sodium chloride per liter); starch LB medium (1 g of starch, 0.5 g of glucose, 10 g of tryptone, 5 g of yeast extract, and 10 g of sodium chloride per liter); starch 0.1LB medium (0.1 g of starch, 0.05 g of glucose, 1 g of tryptone, 0.5 g of yeast extract, and 1 g of sodium chloride per liter); starch medium (1 g of starch, 0.5 g of glucose per liter). All media were prepared with double distilled water and sterilized at 121 °C, 20 min. All microbial seeds were cultured overnight in LB medium at 37 °C.

Microbial Culturing Conditions. Microbes were cultured in LB, 0.1LB, glucose, starch LB, starch 0.1LB, and starch medium with ferric(III)oxide or kaolin ore. Each sample had an initial medium volume of 50 mL, in which 0.3 g of ferric(III)oxide or 1 g of kaolin powder was added and inoculated with the respective microbes to a final optical density of 0.02 (λ = 600 nm). Each culture was in triplicate on a shaker at 160 rpm and room temperature. Samples were taken every 24 h for 14 consecutive days at a rate of 4% of the total volume. The samples were then subjected to biochemical tests. Each experiment included a group of the same condition but without microbes as the negative control.

Ferrous Ion and pH Measurement. Samples taken daily were quick-frozen with liquid nitrogen and stored at −20 °C and finally measured together. The reaction equation of ferrous ion with 1,10-phenanthroline is as follows:

$$Fe^{2+} + 3(phen) = [Fe(phen)_3]^{2+} \quad (1)$$

Ferrous ions can form stable orange complexes with 1,10-phenanthroline.[10] The samples were mixed with 1,10-phenanthroline, ammonium acetate, and sodium fluoride in a ratio of 1:2:2:5 and incubated in the dark under room temperature for 1 h to measure its absorption at 492 nm wavelength through a Tecan microplate reader (Männedorf, Canton of Zurich, Switzerland). The pH was measured directly by a Mettler-Toledo pH meter (Zurich, Canton of Zurich, Switzerland).

Microbial Growth Rate Measurement. Microbial growth rates were measured daily under sterile conditions. The taken samples were diluted with sterile water by 10−20 orders of magnitude according to microbial growth and spread on antibiotic-free LB agar plates. The plates were incubated at 37 °C overnight. The number of colony forming units was recorded according to the number of microbes and dilution ratio.

Determination of Total Ferric(III)oxide Content in Kaolin Clay. Kaolin was treated with 37% (w/v) hydrochloric acid at room temperature for 12 h to convert iron to an ionic state. The resulting solution was mixed with hydroxylamine hydrochloride in a ratio of 1:1 to reduce iron ions, and the concentration of ferrous ions was subsequently determined using 1,10-phenanthroline.

RT-PCR Analysis. The levels of gene expression under different conditions were determined by real-time PCR system (RT-PCR). Sample RNA extraction, reverse transcription into cDNA, and RT-PCR were performed using Promega kits (Madison, Wisconsin, USA) according to the manufacturer's instructions. The quantity and quality of RNA were evaluated by Metash B-500 spectrophotometer (Shanghai, China). The mRNA levels of related genes were determined by Thermo Fisher Scientific real-time PCR system (Waltham, Massachusetts, USA) using BRYT Green dye. The primers were synthesized by Sangon Biotech Co., Ltd. (Shanghai, China). RT-PCR was performed in 20 μL reaction mixture containing 10 μL of GoTaq qPCR Master Mix (contains BRYT Green dye, carboxy-X-rhodamine, GoTaq hot start enzyme, $MgCl_2$, deoxy-ribonucleoside triphosphate, patented reaction buffer), 0.4 μL of forward primer (10 μM), 0.4 μL of reverse primer (10 μM), 0.2 μL of carboxy-X-rhodamine (1×), 7 μL of nuclease-free water, 2 μL of template cDNA. Thermal cycling includes the following conditions: 1 cycle at 95 °C for 10 min, 40 cycles at 95 °C for 15 s and 60 °C for 1 min.

Siderophore Detection. Detection of siderophore in the culture medium was performed by chrome azurol S (CAS) assay.[11] The CAS solution was prepared as follows: Solution No. 1: 0.0027 g of $FeCl_3 \cdot 6H_2O$ was dissolved in 10 mL of HCl of 10 mM. Solution No. 2: 60.5 mg of CAS powder was dissolved in 50 mL of distilled water. Solution No. 3: 4.037 g of piperazine was added to 30 mL of distilled water, followed by 8 mL of concentrated HCl until pH was 5.6 to completely dissolved. Solution No. 4: 21.9 mg of HDTM dissolved in 50 mL of distilled water. 1.5 mL of solution No. 1 was added to 7.5 mL of solution No. 2, mixed with solution Nos. 3 and 4, and brought up to 100 mL using distilled water.

In the CAS assay method, the samples and CAS solution were mixed in equal volumes, and the absorbance of obtained mixture was measured at 630 nm wavelength through microplate reader. The reference blank contained equal volumes of CAS solution and uninoculated medium. The percentage of siderophore units was estimated using the following formula

$$\text{siderophore unit}\ (\%) = \frac{A_r - A_s}{A_r} \times 100 \quad (2)$$

where A_s was the absorbance of the mixture of samples and CAS solution and A_r was the absorbance of the reference blank.

Scanning Electron Microscopy. The morphology of microbes and kaolin was characterized by scanning electron microscopy. The microbes and kaolin were collected by centrifugation at 5000 rpm at room temperature, fixed with 2.5% glutaraldehyde for more than 4 h, and washed two times with 0.1 M phosphate-buffered saline (PBS). The samples were then dehydrated over a graded ethanol series (30%, 50%, 70%, 90%, and 100%) and dried at room temperature overnight. Finally, the samples were visualized on HITACHI Regulus 8100 scanning electron microscope (Tokyo, Japan).

Determination of Microbial Biofilm Formation. Glass surfaces with microbial biofilm growth were stained with crystal violet solution (1 g/L) for 30 min followed by vigorous washing with distilled water twice. The stained surface was dried at 60 °C for 10 h and then suspended in 10 mL of absolute ethanol. The resulting solution was measured at an absorption wavelength of 595 nm.

RESULTS AND DISCUSSION

Based on an earlier study, we identified two Gram-positive bacteria that reduce iron differently compared to Gram-negative bacteria.[12] We further found that the ferric(III)oxide reduction ability of the Gram-positive bacteria *B. cereus* and *S. aureus* are nutrient-dependent. Nitrogen-rich environments elicit microbial ferric reduction by ammonia biosynthesis that raises the media pH. In this study, we further evaluate the ferric(III)oxide reduction ability and its impact on other

https://doi.org/10.1021/acsomega.2c03413
ACS Omega 2022, 7, 37212−37220

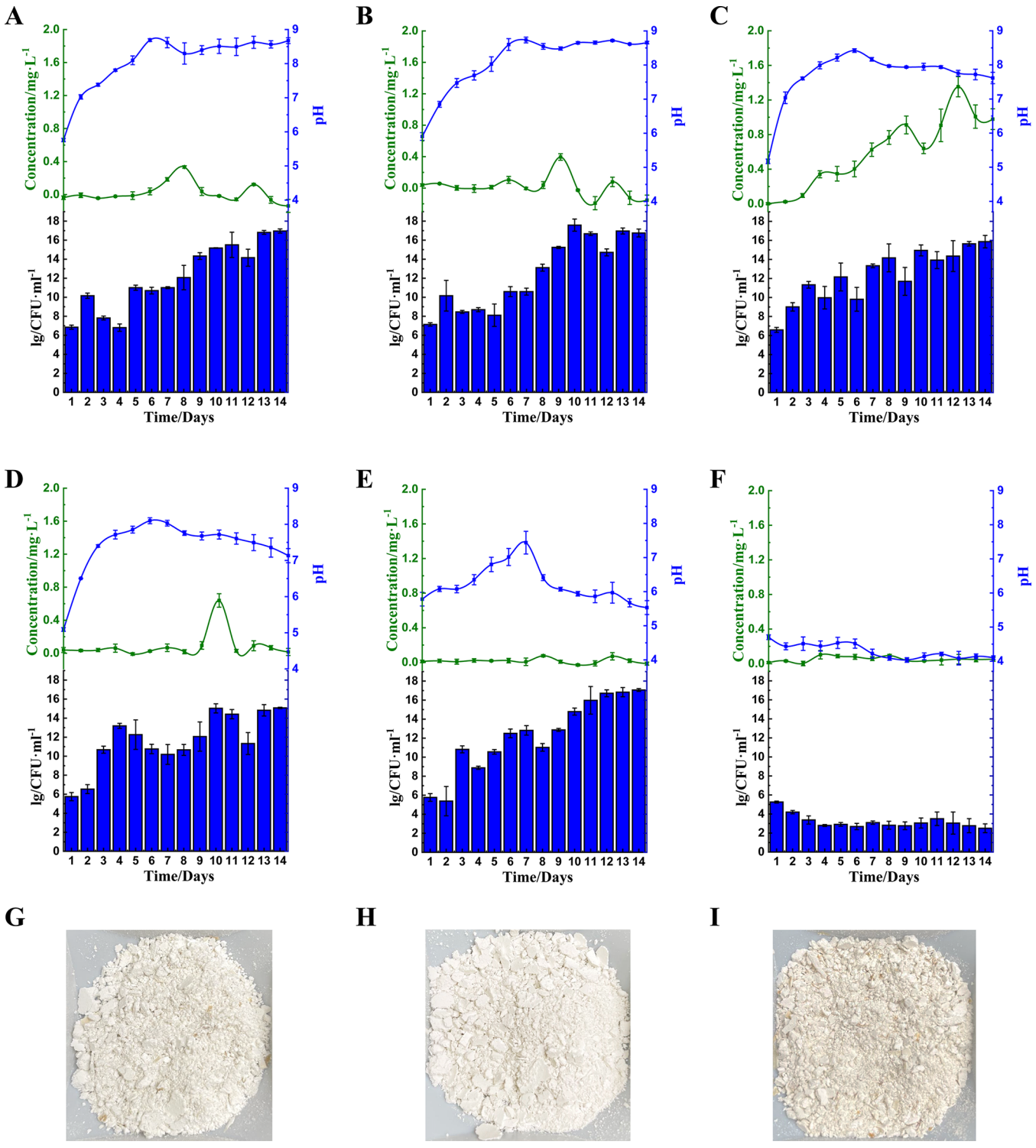

Figure 1. *B. cereus* ferric(III) oxide reduction in starch LB, starch 0.1LB, and starch glucose medium. (A) Fe_2O_3-LB-starch, (B) kaolin-LB-starch, (C) Fe_2O_3-0.1LB-starch, (D) kaolin-0.1LB-starch, (E) Fe_2O_3-glucose-starch, (F) kaolin-glucose-starch. The retrieved kaolin clay after incubation including (G) LB-starch, (H) 0.1LB-starch, (I) glucose-starch. [(green line): ferrous ion concentration; (blue line): pH value, and bar chart: $\log_{10}$ CFU·mL^{-1}. n = 3 independent experiments; mean ± s.d.].

microbial behavior (pH and microbial growth rate) by altering the carbon sources complemented with a nitrogen-rich medium. Generally, ferric(III)oxide salts exist in the α-ferric(III)oxide crystalline form, whereas in kaolin clay, ferric contaminants exist in the form of crystalline ferric(III)oxide and amorphous ferric(III) oxide. Therefore, the iron-reducing ability of *B. cereus* and *S. aureus* was tested on ferric(III) oxide salt (Fe_2O_3) and kaolin. We altered the nitrogen source in the culturing media using either 0×, 0.1×, or 1× lysogeny broth (LB) as a culturing base, supplemented with carbon sources of starch (0.1% w/v) or glucose (0.05% w/v).

Ferric Reduction Properties of *B. cereus*. We found that *B. cereus* cultured with starch showed a slightly weaker degree of alkalization (Figure 1, Figure S1). *B. cereus* cultured in

https://doi.org/10.1021/acsomega.2c03413
ACS Omega 2022, 7, 37212−37220

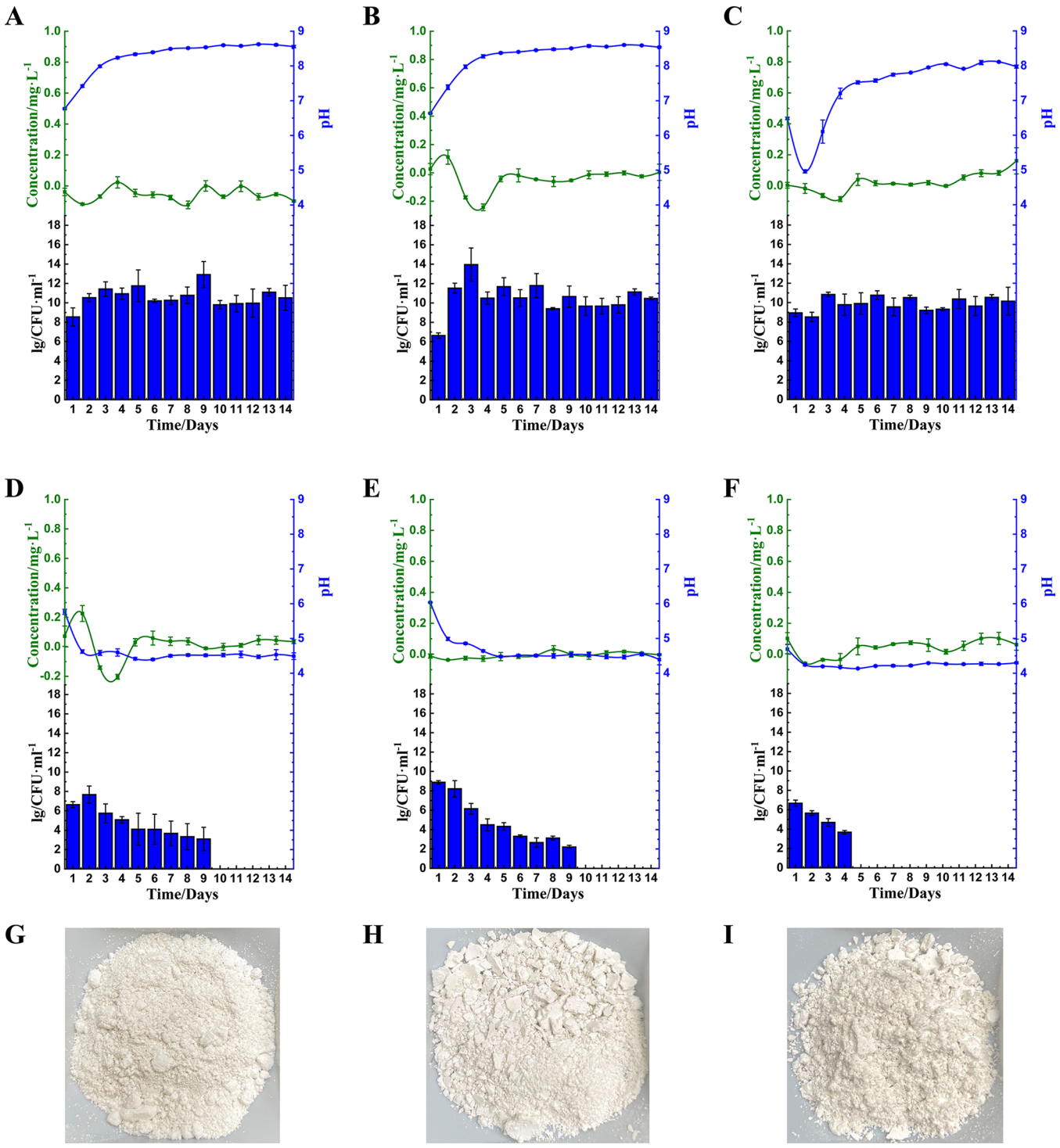

Figure 2. *S. aureus* ferric(III) oxide reduction in starch LB, starch 0.1LB, and starch glucose medium. (A) Fe_2O_3-LB-starch, (B) kaolin-LB-starch, (C) Fe_2O_3-0.1LB-starch, (D) kaolin-0.1LB-starch, (E) Fe_2O_3-glucose-starch, (F) kaolin-glucose-starch. The retrieved kaolin clay after incubation including (G) LB-starch, (H) 0.1LB-starch, (I) glucose-starch. [(green line): ferrous ion concentration; (blue line): pH value, and bar chart: $\log_{10}$ CFU·mL^{-1}. n = 3 independent experiments; mean ± s.d.]

nitrogen-rich media (1× and 0.1× LB) actively reduces crystalline ferric(III) oxide (Figure S1), whereas cultures in starch supplemented media showed a substantial reduction of ferric contaminants in kaolin (Figure 1B,D). Conversely, *B. cereus* in 0.1LB-starch showed the best reduction of Fe_2O_3 (maximum value: 1.2 mg/L) (Figure 1C) and ferric iron in kaolin (up to 0.6 mg/L) (Figure 1D). The cultures in carbon-based media (starch or glucose only) trigger acidification, with the pH decreasing to approximately pH 4 within 24 h of culturing, affecting the growth of *B. cereus* (Figure 1E,F, Figure S1E,F). The presence of Fe_2O_3 negated the media acidification on *B. cereus*, maintaining a close to neutral pH in the medium within the first week, sustaining the *B. cereus* growth. However, we observed no iron reduction presented by the microbe under the culturing condition. Under the best performing conditions, cultures in 0.1LB-starch removed 70.3% of the total ferric(III)

https://doi.org/10.1021/acsomega.2c03413
ACS Omega 2022, 7, 37212−37220

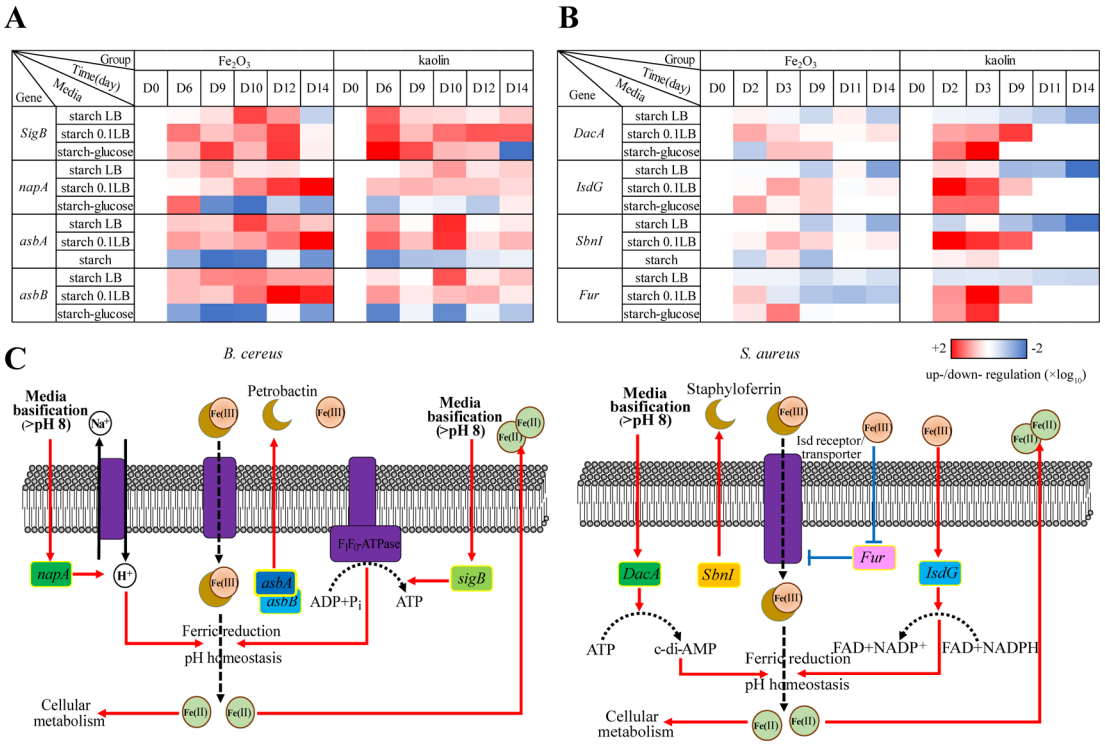

Figure 3. qPCR results and pathway: (A) gene expression of *B. cereus*, (B) gene expression of *S. aureus*, (C) pathway of *B. cereus* (left) and *S. aureus* (right). (Initial qPCR data are available in the Supporting Information).

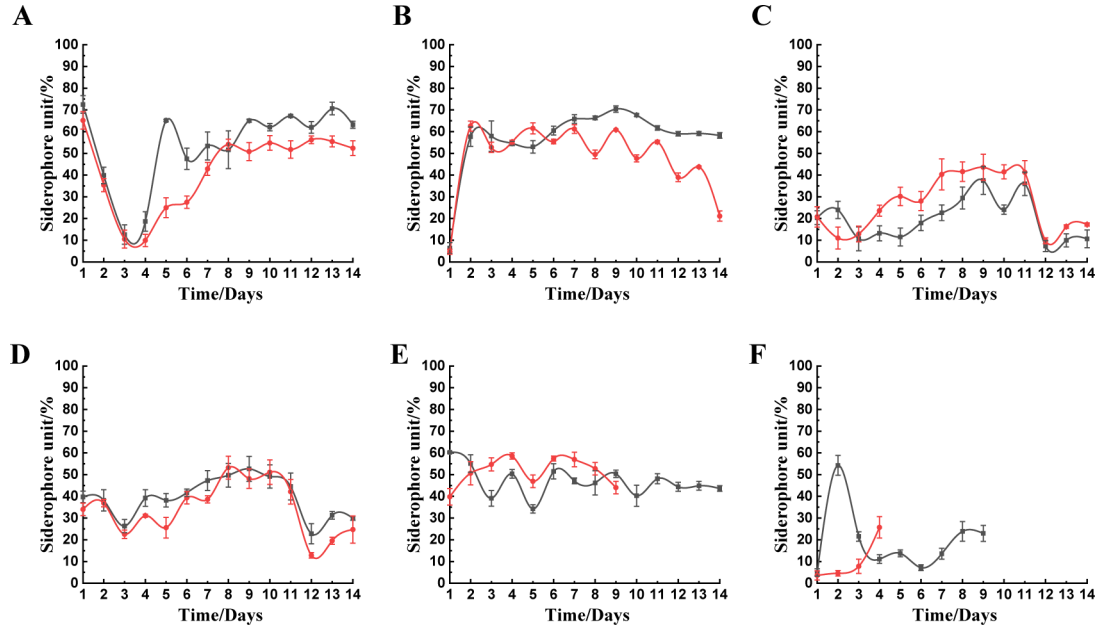

Figure 4. Siderophores produced by *B. cereus* and *S. aureus* in starch LB, starch 0.1LB, and starch glucose medium: (A) *B. cereus*-LB-starch, (B) *B. cereus*-0.1LB-starch, (C) *B. cereus*-glucose-starch, (D) *S. aureus*-LB-starch, (E) *S. aureus*-0.1LB-starch, (F) *S. aureus*-glucose-starch. [(black line): Fe_2O_3; (red line): kaolin. n = 3 independent experiments; mean ± s.d.].

oxide contaminants (Figure 1H), whereas LB-starch and glucose-starch cultures removed 40.2% and 7.1%, respectively (Figure 1G,I). We found that *B. cereus* exerts a homeostatic pH balance, particularly in the presence of iron. *B. cereus* uses carbon-based nutrients to acidify the environment to sustain an ideal pH under a basic environment. Under a limited carbon environment, *B. cereus* readily releases intracellular protons to sustain the homeostatic balance. Based on our results, the use of nitrogen-rich media supplemented with sugar-based nutrients (starch or glucose) further improved the uptake of ferric ions by *B. cereus* in both crystalline and amorphous iron samples.

Ferric Reduction Properties of *S. aureus*. *S. aureus* generates a basic environment in nitrogen-rich cultures (with or without carbon sources), whereas *S. aureus* grown in only carbon-based media resulted in medium acidification within 3

https://doi.org/10.1021/acsomega.2c03413
ACS Omega 2022, 7, 37212−37220

days of incubation (Figure 2A,B,E,F, Figure S2). Interestingly, the use of 0.1× LB showed different pH profiles when cultured with either Fe_2O_3 or kaolin, showing basification and acidification, respectively, affecting the ferric reducing ability of *S. aureus* (Figure 2C,D). *S. aureus* reduces ferric contaminants in kaolin when cultured in both LB-starch and 0.1LB-starch and achieved the maximum reduction within 2 days of culture (Figure 2B,D). In contrast, *S. aureus* cultured in 0.1LB-starch medium showed 2-fold lower Fe_2O_3 reduction (Figure 2C). Similar to *B. cereus*, starch and glucose cultures rapidly acidify to about pH 4, inhibiting *S. aureus* growth and thus no ferric reduction (Figure 2E,F, Figure S2E,F). We found that *S. aureus* cultured in LB-starch, 0.1LB-starch, and glucose-starch removed 29.7%, 32.5%, and 5.9% of ferric(III)oxide contaminants, respectively (Figure 2G−I).

Transcriptomics Analysis of *B. cereus* Bioleaching Mechanism. In order to better follow the cellular processes involved in microbial-mediated bioleaching, we investigated the iron reduction-related genes of *B. cereus* and *S. aureus* under different media conditions (Figure 3). The *B. cereus*'s *asb* gene cluster is responsible for the biosynthesis of the catecholate siderophore, petrobactin, which plays an essential role in intracellular ferric iron transport. These siderophores can be used to reduce oxidative stress while increasing iron acquisition and virulence.[13−15] We observed that *B. cereus* cultured in starch-supplemented nitrogen-rich media (0.1× and 1× LB) showed an up-regulation of *asb* gene cluster (Figure 3A), consistent with the increased siderophores and ferrous ion concentration resulting from the bioleaching process of both Fe_2O_3 and kaolin ores. This phenomenon is evident in *B. cereus* cultured under 0.1LB-starch-Fe_2O_3 conditions, where an approximately 10-fold increase in the *asb* gene cluster expression was observed during the highest concentration of the leached ferrous ion. The siderophore content in these conditions increased rapidly and stabilized at approximately 60% at the beginning of the culture, almost reaching the maximum value of all culture conditions (Figure 4B). Similarly, cultures in the absence of starch (0.1LB-Fe_2O_3) also increased the *asb* gene cluster expression during the highest ferrous ion concentration, while the siderophore content reached approximately 60% (Figures S1, S3, and S8). Interestingly, the addition of any carbon-based nutrients (glucose or starch) triggers the acidification of the surrounding medium (Figure 1E,F, S1E,F).

The *B. cereus*'s *sigB* and *napA* regulate intracellular and extracellular homeostasis. *sigB* was upregulated in *B. cereus* in the presence of kaolin ores or Fe_2O_3 regardless of the culturing condition resultant from the microbial iron metabolism. *B. cereus* grown in nitrogen-rich and carbon-rich media produces various byproducts that alter the surrounding pH, leading to stress response factor expression of *sigB* and Na^+/H^+ antiporter *napA*. These two stress response factors regulate cellular ATP and Na^+/H^+ homeostasis.[16,17] Alternatively, *Bacilli* can metabolize nitrogen-rich nutrients to produce ammonia that basifies the surrounding medium.[18−20] Conversely, simple sugars such as glucose are metabolized through the glycolytic pathway to produce pyruvate and soluble carbon dioxide that acidifies the surrounding medium.[21,22] Complex polysaccharides such as starch are first hydrolyzed to produce dextrin, later converted to monosaccharides used in bacterial metabolism.[22] The slow process of hydrolyzing these polysaccharides influences the gradual acidification of the surrounding media, as observed in the earlier described results (Figure 1A−D). *napA* imports H^+ into the cellular cytoplasm to maintain intracellular homeostasis, providing conducive conditions for ferric ion reduction. Basic pH levels upregulate *napA*, where cultures in 0.1LB-starch-Fe_2O_3 measured a 100-fold increase in *napA* expression, showing the best ferric bioleaching compared to the other culturing conditions (Figure 1C). Similarly, cultures of 0.1LB-Fe_2O_3 showed upregulated *napA* levels during the peak of the iron reduction process (Figures S1C and S3A). The acidic environment generated by cultures in sugar-based media down-regulates *napA* expression by 100-fold. These results are indicative of the role of *napA* in regulating the homeostatic balance of pH in the environment.

Transcriptomics Analysis of *S. aureus* Bioleaching Mechanism. We similarly investigated the various *S. aureus* genes involved in iron reduction, including the iron-regulated surface determinant (Isd) system (ferric transport and internalization), *SbnI* (siderophore biosynthesis), and *DacA* (pH homeostasis). We observed minimal changes in *IsdG* expression from *S. aureus* cultured in LB-starch media despite showing no impairment to the bacterial growth. In contrast, lowered nitrogen-based nutrition was found to upregulate *IsdG* approximately 100-fold in 0.1LB-starch cultures while inhibiting growth, affecting ferric bioleaching in kaolin clay cultures (Figure 3B). Similarly, the *S. aureus* cultures in 0.1LB exhibited a good ferric reduction in Fe_2O_3 while upregulating *IsdG* (Figure S3B). We further observed *SbnI* up-regulation by 100-fold in 0.1LB-starch-kaolin and 0.1LB-Fe_2O_3. *SbnI* regulates the ferric binding siderophore staphyloferrin biosynthesis, facilitating ferric internalization.[23,24] The ferric-bound staphyloferrin is then reduced by iron uptake oxidoreductase (IruO), a flavin adenine dinucleotide (FAD)-containing nicotinamide adenine dinucleotide phosphate (NADPH)-dependent reductase.[25,26] Therefore, corresponding to the up-regulation of *SbnI*, it can be seen that the siderophores content reached a high stable level of approximately 50% in 0.1LB-starch (Figure 4E). About 50% of siderophores in the nitrogen-rich medium were also maintained in 0.1LB (Figure S8E).

Just as in *B. cereus* cultures, *S. aureus* cultures can alter the surrounding pH by using different nutrients. *DacA*, a membrane-bound diadenylate cyclase, is upregulated in *S. aureus* under an acidic environment to produce cyclic di-AMP that triggers nitrogen metabolism to restore normal cell function and ferric iron transport. In sugar-based media (starch and glucose), *DacA* was upregulated by 100-fold attributed to the acidification of the media (Figures 3B and S3B). The addition of starch to 0.1LB also showed acidification of the media while upregulating *DacA*, which is attributed to the *S. aureus*'s ability to rapidly break down starch to glucose. Generally, *S. aureus* upregulates Isd proteins via ferric uptake repressor (Fur) inactivation in the presence of iron.[27] The down-regulation of *Fur* is often observed in *S. aureus* cultured under an iron-reducing environment. Intriguingly, we observed that *Fur* up-regulation in the presence of starch, regardless of the state of the microbial growth or the leached iron profile, except for *S. aureus* grown in a glucose solution, where no readout was observed due to poor microbial viability (Figure S3B).

Microbial Localization on Kaolin Ores. Earlier studies also showed that microbial localization on mineral ores plays a crucial role in facilitating iron reduction, giving rise to the fundamental question of the ability of these two microbes to localize on the surface of the kaolin clay to facilitate iron internalization and reduction.[28] We discovered that the

https://doi.org/10.1021/acsomega.2c03413
ACS Omega 2022, 7, 37212−37220

different culturing conditions also affect microbial localization and biofilm formation on the clay surface (Figure S9). The accumulated biofilm produced by *B. cereus* cultured in LB and glucose medium showed 2-fold higher compared to 0.1LB medium (Figure 5A). Contrariwise, *B. cereus* and *S. aureus*

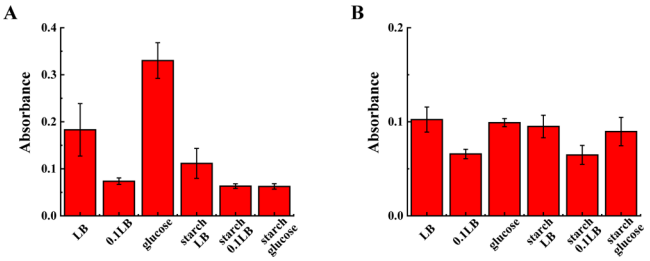

Figure 5. Biofilm growth of (A) *B. cereus* and (B) *S. aureus* under different culturing conditions. Photographs of biofilm growth and staining are available in the Supporting Information. (n = 3 independent experiments; mean ± s.d.)

produced the least biofilm under 0.1LB and starch 0.1LB compared to other conditions (Figure 5), attributed to the excessive microbial growth in nutrient-rich medium such as LB medium. In the presence of a simple carbon source, the acidification of the surrounding environment coupled with the lack of growth essential nutrients promote biofilm formation. Intriguingly, the addition of complex sugars such as starch inhibited the biofilm formation but increased its iron-reducing ability. These observations were consistent with our scanning electron microscopy visualized images of microbial localization on the mineral surface (Figure 6). We observed the biofilm

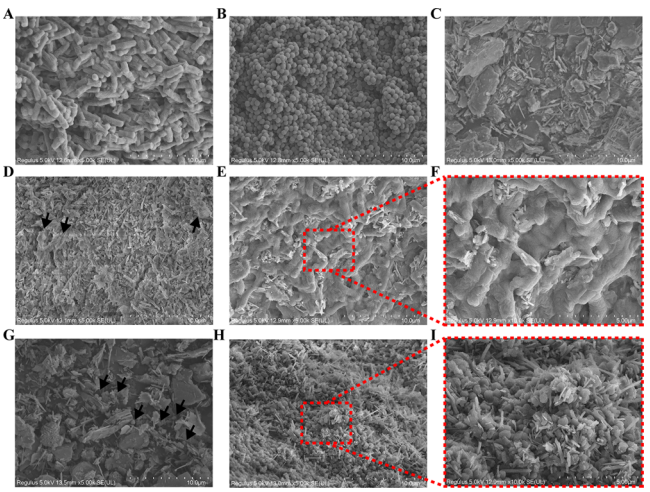

Figure 6. Scanning electron microscopic images of microbes and kaolin: (A) *B. cereus*, (B) *S. aureus*, (C) kaolin, (D) kaolin with low concentrations of *B. cereus*, (E) kaolin with high concentrations of *B. cereus*, (F) high magnification of kaolin with high concentrations of *B. cereus*, (G) kaolin with low concentrations of *S. aureus*, (H) kaolin with high concentrations of *S. aureus*, (I) high magnification of kaolin with high concentrations of *S. aureus*.

formation of both microbes cultured with kaolin ore for 24 h at room temperature under low ($OD_{600\ nm}$: <0.5) and high ($OD_{600\ nm}$: >1.5) cellular density in nutrient sufficient medium. Low cellular density of *B. cereus* showed scattered microbial microcolonies on the kaolin ores, increasing the microbial microcolonies and kaolin ore contact area (Figure 6D). With higher *B. cereus* density, we observed extensive biofilm formation that completely covers the surface of the kaolin ores (Figure 6E). Similarly, the low cellular density *S. aureus* inoculum showed dispersed microcolonies formation on the kaolin ore (Figure 6G), while higher starting *S. aureus* density also showed extensive biofilm formation on the ore surface (Figure 6H). Various literature reports have illustrated the role of biofilm-forming communities in facilitating the iron acquisition and iron reduction. Various Gram-negative and Gram-positive bacteria such as *Pseudomonas aeruginosa*, *Campylobacter jejuni*, and *Staphylococcus aureus* cause iron corrosion by readily forming biofilm on the iron surfaces. The rate of iron corrosion was much slower in planktonic microbial cultures due to ineffective microbial iron metabolism.[29−31] Based on our current experimental results, a controlled level of biofilm mass facilitates better iron reduction, allowing microbial localization on the clay surface for effective iron reduction. Excessive biofilm mass would hinder the contact between microbes and clay, thus reducing the iron-reducing ability. Therefore, moderate biofilm formation through regulating the media composition can further enhance the microbial iron metabolism on kaolin ores.

CONCLUSIONS

In conclusion, we investigated the iron reduction mechanism of Gram-positive bacteria under different culture conditions. We discovered that Gram-positive bacteria *B. cereus* and *S. aureus* use nitrogen sources to increase the medium's pH, facilitating the iron reduction process by regulating intracellular pH homeostasis and bacterial growth. Meanwhile, the level of biofilm formation was also found to affect iron reduction. This work established the connection of the various genes in regulating the microbial bioleaching process. It helps understand the microbial iron leaching process that enables the screening of other Gram-positive bacteria exhibiting good iron-reduction ability in the future. This discovery sets the stage for further development of engineered microbes that can more effectively and cleanly remove iron contaminants from samples.

ASSOCIATED CONTENT

Supporting Information

The Supporting Information is available free of charge at https://pubs.acs.org/doi/10.1021/acsomega.2c03413.

Nine figures and one table encompassing the ferric(III)-oxide reduction of the different Gram-positive bacteria in different media, the qPCR results and analysis of the microbial expressed genes, the microbial siderophore production levels, and the biofilm growth, along with the corresponding images documenting these changes (PDF)

AUTHOR INFORMATION

Corresponding Authors

Jun Chen − *Department of Biomedical Engineering, Southern University of Science and Technology (SUSTech), Shenzhen 518055, China; Shenzhen Institute of Synthetic Biology, Shenzhen Institutes of Advanced Technology (SIAT), Chinese Academy of Sciences, Shenzhen 518055, China*; Email: chenj3@sustech.edu.cn, j.chen@siat.ac.cn

Chun Loong Ho − *Department of Biomedical Engineering, Southern University of Science and Technology (SUSTech), Shenzhen 518055, China; Shenzhen Institute of Synthetic*

https://doi.org/10.1021/acsomega.2c03413
ACS Omega 2022, 7, 37212−37220

Biology, Shenzhen Institutes of Advanced Technology (SIAT), Chinese Academy of Sciences, Shenzhen 518055, China; orcid.org/0000-0003-2846-3392; Email: hejl@sustech.edu.cn, cl.ho@siat.ac.cn

Authors

Hao Jing − *Department of Biomedical Engineering, Southern University of Science and Technology (SUSTech), Shenzhen 518055, China*

Zhao Liu − *Department of Biomedical Engineering, Southern University of Science and Technology (SUSTech), Shenzhen 518055, China*

Complete contact information is available at: https://pubs.acs.org/10.1021/acsomega.2c03413

Author Contributions

C.L.H. and J.C. designed the study. H.J. and Z.L. performed the experiments. C.L.H, J.C., and H.J. analyzed the data. C.L.H. and J.C. wrote the manuscript. C.L.H. supervised the project. All authors discussed the results and commented on the manuscript.

Funding

This project is financially supported by the National Natural Science Foundation of China's Research Fund for International Young Scientists (22050410270), the Shenzhen Special Fund for Innovation and Entrepreneurship of Overseas High-level Talents Peacock Team (KQTD20170810111314625), and the Guangdong Innovative and Entrepreneurial Research Team Program (2019ZT08Y191).

Notes

The authors declare no competing financial interest.

■ ACKNOWLEDGMENTS

The authors wish to thank Xinyi Chen for her assistance with the manuscript. The authors also wish to thank the advice provided by Seng How Kuan and Sylvia Chieng.

■ REFERENCES

(1) Lee, E. Y.; Cho, K.-S.; Wook Ryu, H. Microbial refinement of kaolin by iron-reducing bacteria. *Appl. Clay Sci.* **2002**, *22*, 47−53.

(2) Murray, H. H.Structure and composition of the clay minerals and their physical and chemical properties. In *Developments in Clay Science*; Murray, H. H., Ed.; Elsevier, 2006; Chapter 2, pp 7−31.

(3) He, Q.-x.; Huang, X.-c.; Chen, Z.-L. Influence of organic acids, complexing agents and heavy metals on the bioleaching of iron from kaolin using Fe(III)-reducing bacteria. *Appl. Clay Sci.* **2011**, *51*, 478−483.

(4) de Mesquita, L. M. S.; Rodrigues, T.; Gomes, S. S. Bleaching of Brazilian kaolins using organic acids and fermented medium. *Miner. Eng.* **1996**, *9*, 965−971.

(5) Cameselle, C.; Ricart, M. T.; Núñez, M. J.; Lema, J. M. Iron removal from kaolin. Comparison between "in situ" and "two-stage" bioleaching processes. *Hydrometallurgy* **2003**, *68*, 97−105.

(6) Hau, H. H.; Gralnick, J. A. Ecology and biotechnology of the genus *Shewanella*. *Annu. Rev. Microbiol.* **2007**, *61*, 237−258.

(7) Kostka, J. E.; Stucki, J. W.; Nealson, K. H.; Wu, J. Reduction of structural Fe(III) in smectite by a pure culture of *Shewanella Putrefaciens* strain MR-1. *Clays Clay Miner.* **1996**, *44*, 522−529.

(8) Nealson, K. H.; Saffarini, D. Iron and manganese in anaerobic respiration: environmental significance, physiology, and regulation. *Annu. Rev. Microbiol.* **1994**, *48*, 311−343.

(9) Nealson, K. H.; Myers, C. R. Microbial reduction of manganese and iron: new approaches to carbon cycling. *Appl. Environ. Microbiol.* **1992**, *58*, 439−443.

(10) Fadrus, H.; Malý, J. Suppression of iron(III) interference in the determination of iron(II) in water by the 1,10-phenanthroline method. *Analyst* **1975**, *100*, 549−554.

(11) Payne, S. M.Detection, isolation, and characterization of siderophores. In *Bacterial Pathogenesis, Part A: Identification and Regulation of Virulence Factors*; Clark, V. L., Bavoil, P. M., Eds.; Academic Press, 1994; Chapter 25, pp 329−344.

(12) Jing, H.; Liu, Z.; Kuan, S. H.; Chieng, S.; Ho, C. L. Elucidation of Gram-Positive Bacterial Iron(III) Reduction for Kaolinite Clay Refinement. *Molecules* **2021**, *26*, 3084.

(13) Dixon, S. D.; Janes, B. K.; Bourgis, A.; Carlson, P. E., Jr.; Hanna, P. C. Multiple ABC transporters are involved in the acquisition of petrobactin in *Bacillus anthracis*. *Mol. Microbiol.* **2012**, *84*, 370−382.

(14) Wilson, M. K.; Abergel, R. J.; Raymond, K. N.; Arceneaux, J. E. L.; Byers, B. R. Siderophores of *Bacillus anthracis*, *Bacillus cereus*, and *Bacillus thuringiensis*. *Biochem. Biophys. Res. Commun.* **2006**, *348*, 320−325.

(15) Koppisch, A. T.; Dhungana, S.; Hill, K. K.; Boukhalfa, H.; Heine, H. S.; Colip, L. A.; Romero, R. B.; Shou, Y.; Ticknor, L. O.; Marrone, B. L.; Hersman, L. E.; Iyer, S.; Ruggiero, C. E. Petrobactin is produced by both pathogenic and non-pathogenic isolates of the *Bacillus cereus* group of bacteria. *BioMetals* **2008**, *21*, 581−589.

(16) Desriac, N.; Broussolle, V.; Postollec, F.; Mathot, A.-G.; Sohier, D.; Coroller, L.; Leguerinel, I. *Bacillus cereus* cell response upon exposure to acid environment: toward the identification of potential biomarkers. *Front. Microbiol.* **2013**, *4*, 284−284.

(17) Padan, E.; Venturi, M.; Gerchman, Y.; Dover, N. Na^+/H^+ antiporters. *Biochim. Biophys. Acta* **2001**, *1505*, 144−157.

(18) Cepl, J.; Blahůšková, A.; Cvrčková, F.; Markoš, A. Ammonia produced by bacterial colonies promotes growth of ampicillin-sensitive *Serratia* sp. by means of antibiotic inactivation. *FEMS Microbiol. Lett.* **2014**, *354*, 126−132.

(19) Navarro Llorens, J. M.; Tormo, A.; Martínez-García, E. Stationary phase in gram-negative bacteria. *FEMS Microbiol. Rev.* **2010**, *34*, 476−495.

(20) Farrell, M. J.; Finkel, S. E. The growth advantage in stationary-phase phenotype conferred by *rpoS* mutations is dependent on the pH and nutrient environment. *J. Bacteriol.* **2003**, *185*, 7044−7052.

(21) Lovley, D. R. Dissimilatory Fe(III) and Mn(IV) reduction. *Microbiol. Rev.* **1991**, *55*, 259−287.

(22) Guo, M.-r.; Lin, Y.-m.; Xu, X.-p.; Chen, Z.-l. Bioleaching of iron from kaolin using Fe(III)-reducing bacteria with various carbon nitrogen sources. *Appl. Clay Sci.* **2010**, *48*, 379−383.

(23) Conroy, B. S.; Grigg, J. C.; Kolesnikov, M.; Morales, L. D.; Murphy, M. E. P. *Staphylococcus aureus* heme and siderophore-iron acquisition pathways. *BioMetals* **2019**, *32*, 409−424.

(24) Verstraete, M. M.; Morales, L. D.; Kobylarz, M. J.; Loutet, S. A.; Laakso, H. A.; Pinter, T. B.; Stillman, M. J.; Heinrichs, D. E.; Murphy, M. E. P. The heme-sensitive regulator SbnI has a bifunctional role in staphyloferrin B production by *Staphylococcus aureus*. *J. Biol. Chem.* **2019**, *294*, 11622−11636.

(25) Zhou, C.; Fey, P. D. The acid response network of *Staphylococcus aureus*. *Curr. Opin. Microbiol.* **2020**, *55*, 67−73.

(26) Bowman, L.; Zeden, M. S.; Schuster, C. F.; Kaever, V.; Gründling, A. New insights into the cyclic di-adenosine monophosphate (c-di-AMP) degradation pathway and the requirement of the cyclic dinucleotide for acid stress resistance in *Staphylococcus aureus*. *J. Biol. Chem.* **2016**, *291*, 26970−26986.

(27) Zapotoczna, M.; Jevnikar, Z.; Miajlovic, H.; Kos, J.; Foster, T. J. Iron-regulated surface determinant B (IsdB) promotes *Staphylococcus aureus* adherence to and internalization by non-phagocytic human cells. *Cell. Microbiol.* **2013**, *15*, 1026−1041.

(28) Yong, S. N.; Lim, S.; Ho, C. L.; Chieng, S.; Kuan, S. H. Mechanisms of microbial-based iron reduction of clay minerals: Current understanding and latest developments. *Appl. Clay Sci.* **2022**, *228*, 106653.

(29) Li, J.; Nickel, R.; Wu, J.; Lin, F.; van Lierop, J.; Liu, S. A new tool to attack biofilms: driving magnetic iron-oxide nanoparticles to disrupt the matrix. *Nanoscale* **2019**, *11*, 6905−6915.
(30) Oh, E.; Andrews, K. J.; Jeon, B. Enhanced biofilm formation by ferrous and ferric iron through oxidative stress in *Campylobacter jejuni*. *Front. Microbiol.* **2018**, DOI: 10.3389/fmicb.2018.01204.
(31) Kang, D.; Kirienko, N. V. Interdependence between iron acquisition and biofilm formation in *Pseudomonas aeruginosa*. *J. Microbiol.* **2018**, *56*, 449−457.

https://doi.org/10.1021/acsomega.2c03413
ACS Omega 2022, 7, 37212−37220